RESEARCH PAPER

Development and Evaluation of Luliconazole-Loaded PEG-Coated Silver Nanoparticle Hydrogels for Enhanced Antifungal Activity

Dr. Shailaja V. Jadhav[1*], Dr. Ravindra N. Chintamani[2], Dr. Dhairysheel M. Ghadge[3], Sayali Dalvi[4], Ashish Yadav[5]

[1*]S.N.B.P. College of Pharmacy, Chikhali, Pune, Maharashtra, India.
Email: jshailaja081@gmail.com
[2]S.N.B.P. College of Pharmacy, Chikhali, Pune, Maharashtra, India.
[3]Gourishankar Institute of Pharmaceutical Education & Research, Limb, Satara, Maharashtra, India.
Email: dhairysheelsatara@gmail.com
[4,5]Gourishankar Institute of Pharmaceutical Education & Research, Limb, Satara, Maharashtra, India.
Corresponding Author: Dr. Shailaja V. Jadhav
S.N.B.P. College of Pharmacy, Chikhali, Pune, Maharashtra, India.
Email: jshailaja081@gmail.com

ABSTRACT

Fungal infections, particularly those caused by *Candida albicans*, remain a significant clinical challenge due to the rising incidence of drug resistance and the poor aqueous solubility of current antifungal agents like luliconazole (LZL). This study aimed to develop, optimize, and evaluate a novel topical hydrogel combining PEG-coated luliconazole with green-synthesized silver nanoparticles (AgNPs) to achieve synergistic antifungal activity and enhanced skin permeation. AgNPs were successfully biosynthesized using an aqueous leaf extract of *Epipremnum aureum* as a reducing agent. Formulations were prepared using varying concentrations of Carbopol 940 and HPMC K100, combined with PEG 6000 as a coating/stabilizing agent. The optimized formulation (Carbopol F2: 3% Carbopol, 100 mg PEG 6000, 3 mL AgNPs) exhibited a particle size of 192.0 nm, a zeta potential of -44.7 mV, and a viscosity of 4964 cps. In vitro drug release studies using a Franz diffusion cell showed that Carbopol F2 achieved a maximum cumulative release of 79.04% over 360 minutes, significantly outperforming the formulation without AgNPs (63.67%). Furthermore, the optimized hydrogel demonstrated exceptional antifungal efficacy against *C. albicans* with a zone of inhibition of 33 mm, compared to 8 mm for the pure drug and 11 mm for the control hydrogel. The combination of green-synthesized AgNPs and PEG-coated LZL in a mucoadhesive Carbopol hydrogel represents a highly promising platform for the topical treatment of resistant fungal infections.

Keywords: Luliconazole; Silver Nanoparticles; Green Synthesis; *Epipremnum aureum*; Hydrogel; Antifungal Activity; Topical Drug Delivery.

How to cite this article: Jadhav SV, Chintamani RN, Ghadge DM, Dalvi S, Yadav A. Development and Evaluation of Luliconazole-Loaded PEG-Coated Silver Nanoparticle Hydrogels for Enhanced Antifungal Activity. Int J Drug Deliv Technol. 2026;16(53s): 808-814. DOI: 10.25258/ijddt.16.53s.130

Source of support: Nil.

Conflict of interest: None.

1. Introduction

Topical drug delivery systems offer numerous advantages over oral administration, including the avoidance of hepatic first-pass metabolism, reduced systemic toxicity, and improved patient compliance, particularly in the treatment of localized dermatological conditions [1]. Fungal infections of the skin, such as dermatophytosis and candidiasis, are globally prevalent and their management is increasingly complicated by the emergence of antifungal resistance [2]. Luliconazole (LZL) is a potent, broad-spectrum imidazole antifungal agent that works by inhibiting ergosterol biosynthesis [3]. However, LZL is classified as a Biopharmaceutics Classification System (BCS) Class II drug, characterized by high permeability but poor aqueous solubility (0.0978 mg/mL) [4]. This low solubility severely limits its formulation into effective topical aqueous gels and reduces its bioavailability at the site of infection [5].

To overcome these challenges, nanotechnology has emerged as a transformative strategy. Silver nanoparticles (AgNPs) have garnered immense interest in biomedical applications due to their inherent, broad-spectrum antimicrobial and antifungal properties [6]. AgNPs interact with the fungal cell membrane, disrupting its integrity, inducing the generation of reactive oxygen species (ROS), and interfering with DNA replication [7, 8]. The integration of AgNPs with conventional antifungal drugs has been shown to produce a synergistic effect, effectively lowering the required dose of the drug and mitigating the risk of resistance [9]. However, the traditional chemical synthesis of AgNPs often involves toxic reducing agents. Green synthesis, utilizing plant extracts such as *Epipremnum aureum* (Devil's Ivy), provides an eco-friendly, cost-effective, and biocompatible alternative [10]. The phytochemicals in the extract act as both reducing and stabilizing agents [11].

To further enhance the stability of the nanoparticles and the solubility of LZL, Polyethylene Glycol (PEG) 6000 can be employed as a coating agent. PEGylation provides steric stabilization to the nanoparticles, preventing agglomeration, and acts as a solid dispersion matrix to enhance the dissolution rate of the poorly soluble drug [12, 13]. Finally, formulating these modified active pharmaceutical ingredients

(APIs) into a mucoadhesive hydrogel utilizing polymers like Carbopol 940 or Hydroxypropyl Methylcellulose (HPMC) K100 ensures prolonged residence time on the skin, controlled drug release, and optimal hydration of the stratum corneum [14, 15]. The objective of this study was to systematically develop and evaluate a LZL-loaded, PEG-coated AgNP hydrogel for enhanced topical antifungal delivery.

2. Literature Review

The formulation of BCS Class II drugs for topical application requires innovative approaches. Previous studies have demonstrated the utility of lipid-based nanoparticles, niosomes, and microemulsions to enhance the permeation of LZL [16, 17]. Dandagi et al. [18] reported a microemulsion-based gel for LZL that showed improved *in vitro* release. However, integrating active metallic nanoparticles with organic APIs offers a dual-action mechanism.

The antifungal efficacy of AgNPs is well-documented. Hawar et al. [19] demonstrated strong antifungal activity of green-synthesized AgNPs against *Candida albicans* and *C. glabrata*. The mechanism of action, as elucidated by Lee et al. [20], involves cell membrane disruption, which is highly complementary to LZL's mechanism of inhibiting ergosterol synthesis [21]. The stabilization of AgNPs is critical to maintaining their nano-size and efficacy. Studies by Tejamaya et al. [22] and Pinzaru et al. [23] confirmed that PEG-coated silver nanoparticles exhibit superior stability in biological media and reduced cytotoxicity compared to uncoated or citrate-capped AgNPs.

Hydrogels, owing to their high water content and biocompatibility, are ideal vehicles for topical application. Carbopol 940 and HPMC have been extensively evaluated for their rheological and mucoadhesive properties [24, 25]. A study by Jain et al. [26] highlighted the excellent spreadability and sustained release profile of Carbopol-based hydrogels for transdermal delivery. This research builds upon these established paradigms by combining green-synthesized AgNPs, PEGylation, and hydrogel technology into a single, optimized topical formulation for LZL.

3. Materials and Methods

3.1 Materials

Luliconazole was obtained as a gift sample. Silver nitrate ($AgNO_3$), Carbopol 940, Hydroxypropyl Methylcellulose (HPMC K100), Polyethylene Glycol (PEG 6000), and all other analytical-grade chemicals and solvents (ethanol, methanol, acetone) were procured from SD Chem Lab, Mumbai, India. Fresh leaves of *Epipremnum aureum* were collected locally and authenticated. *Candida albicans* strains were obtained from local microbiological repositories.

3.2 Preformulation Studies

The solubility of LZL was determined in water, acetone, methanol, and ethanol. The melting point was determined using a Thiele's tube assembly. UV-Visible spectroscopy was utilized to determine the maximum absorbance (λ_{max}) and to construct a calibration curve. Stock solutions were prepared, and the calibration curve was plotted over a concentration range of 2–25 µg/mL in ethanol and pH 7.4 phosphate buffer [27]. Fourier Transform Infrared (FTIR) spectroscopy and Differential Scanning Calorimetry (DSC) were performed to confirm drug identity and to assess compatibility between the drug and excipients [28, 29].

3.3 Green Synthesis of Silver Nanoparticles (AgNPs)

An aqueous extract of *Epipremnum aureum* was prepared by washing 10 g of fresh leaves, grinding them into a fine paste, and soaking in 50 mL of sterile Milli-Q water overnight, followed by filtration. For the biosynthesis of AgNPs, 170 mg of $AgNO_3$ was dissolved in 95 mL of water.

To this, 5 mL of the leaf extract was added to serve as the reducing and stabilizing agent. The mixture was heated at 70 °C for 30 minutes. The successful reduction of silver ions was visually indicated by a color change from light green to dark brown [30]. The synthesized AgNPs were characterized using UV-Visible spectroscopy.

3.4 Formulation of LZL-PEG-AgNPs Hydrogels

Luliconazole was coated with PEG 6000 using a solvent-antisolvent precipitation method to enhance its solubility and stability [31]. Briefly, 100 mg of LZL and varying amounts of PEG 6000 (50, 100, or 150 mg) were dissolved in 10 mL of ethanol. This solution was added dropwise to an aqueous base containing the polymer (Carbopol 940 or HPMC K100) while stirring at 50 rpm.

Subsequently, 3 mL of the synthesized AgNP suspension was integrated into the mixture. The formulations containing Carbopol were neutralized with a few drops of 0.1 N Sodium Hydroxide (NaOH) to facilitate gelation. Six main formulations were prepared alongside a control (optimized batch without AgNPs), as detailed in Table 1.

Table 1: Composition of LZL-PEG-AgNPs Hydrogel Formulations

Batch Code	Polymer Type	Polymer Conc. (%)	LZL (mg)	PEG 6000 (mg)	AgNPs (mL)
Ca. F1	Carbopol 940	2	100	50	3

Ca. F2	Carbopol 940	3	100	100	3
Ca. F3	Carbopol 940	4	100	150	3
HPMC F1	HPMC K100	2	100	50	3
HPMC F2	HPMC K100	3	100	100	3
HPMC F3	HPMC K100	4	100	150	3

3.5 Characterization of Hydrogels

Dynamic Light Scattering (DLS) was used to determine the particle size, Polydispersity Index (PDI), and zeta potential of the nanogels [32]. Viscosity was measured using a Brookfield Viscometer (Spindle L4 at 100 rpm). The pH of the formulations was determined using a calibrated digital pH meter. Spreadability was evaluated using the "slip and drag" method [33]. Drug content was analyzed by extracting the drug in ethanol, sonicating, filtering, and measuring absorbance spectrophotometrically.

3.6 *In vitro* Drug Release and Antifungal Activity

In vitro drug permeation was evaluated over 360 minutes using a Franz diffusion cell with a phosphate buffer (pH 7.4) receptor medium maintained at 37 °C [34]. Antifungal efficacy against *C. albicans* was determined utilizing the agar well-diffusion method. The zones of inhibition were measured in millimeters (mm) after incubation [35].

4. Results

4.1 Preformulation and Compatibility Studies

The solubility of LZL was confirmed to be practically insoluble in water (0.0978 mg/mL), freely soluble in acetone, and slightly soluble in methanol and ethanol. The melting point was recorded at 150-154 °C. The λ_{max} was observed at 295 nm, and the calibration curves exhibited excellent linearity (R^2 = 0.990 in ethanol; R^2 = 0.991 in pH 7.4 buffer). FTIR analysis of pure LZL showed characteristic peaks at 3028.99 cm^{-1} (C-H stretch), 1552.36 cm^{-1} (C=C stretch), 1365.44 cm^{-1} (C-H stretch), 1048.91 cm^{-1} (S=O stretch), and 759.70 cm^{-1} (C-Cl stretch). The physical mixture maintained these core functionalities with slight shifts (e.g., 3341.41 cm^{-1}, 1636.68 cm^{-1}, 1271.02 cm^{-1}, 1050.72 cm^{-1}, and 647.32 cm^{-1}), confirming the absence of adverse chemical interactions. DSC thermograms of pure LZL displayed a sharp endothermic peak between 150-154 °C, which shifted significantly to approximately 112 °C in the physical mixture, indicating successful entrapment and amorphization of the drug within the PEG/polymer matrix.

4.2 Synthesis and Characterization of AgNPs

The green synthesis of AgNPs was visibly confirmed by the transition of the reaction mixture from light green to dark brown. UV-Vis spectroscopy revealed a distinct surface plasmon resonance peak at 219 nm. DLS characterization of the raw AgNPs indicated a mean particle size of 141.7 nm, a very narrow PDI of 0.039, and a highly stable zeta potential of -25.9 mV, suggesting strong electrostatic repulsion preventing aggregation.

4.3 Nanoparticle Size and Zeta Potential in Formulations

Table 2 summarizes the particle size, PDI, and zeta potential of the formulated hydrogels. The Carbopol F2 batch exhibited the most favorable nanoparticle dimensions (192.0 nm) and the highest absolute zeta potential (-44.7 mV), indicating superior colloidal stability.

Table 2: Particle Size, PDI, and Zeta Potential of Hydrogel Formulations

Formulation	Particle Size (nm)	PDI	Zeta Potential (mV)
Ca. F1	276.5	0.304	-43.3
Ca. F2	192.0	0.495	-44.7
Ca. F3	350.0	0.421	-40.7
HPMC F1	299.1	0.587	-42.5
HPMC F2	250.0	0.421	-42.3
HPMC F3	276.5	0.304	-40.0

4.4 Physicochemical Evaluation of Hydrogels

All formulations displayed pH values ranging from 6.43 to 7.17, which falls well within the acceptable physiological range for skin application (pH 4.5–7.5), minimizing the risk of irritation. The drug content was uniformly high across all batches, ranging from 84.78% to 96.76%, with Ca. F2 exhibiting the highest encapsulation efficiency. Viscosity and spreadability are critical parameters for topical application. As

polymer concentration increased, viscosity increased while
spreadability decreased. The Ca. F2 batch provided an optimal balance, ensuring the gel could be easily applied while maintaining sufficient structural integrity for sustained release (Table 3).

Table 3: Physicochemical Properties of Hydrogels

Formulation	Drug Content (%)	Viscosity (cps)	pH	Spreadability (g·cm/sec)
Ca. F1	90.21	4401	6.52	7.96
Ca. F2	96.76	4964	6.43	6.32
Ca. F3	93.47	4551	6.65	7.25
HPMC F1	86.95	3890	7.04	9.37
HPMC F2	84.78	4193	7.12	8.63
HPMC F3	92.39	4470	7.17	9.55
Control (No AgNPs)	88.04	4745	6.80	6.71

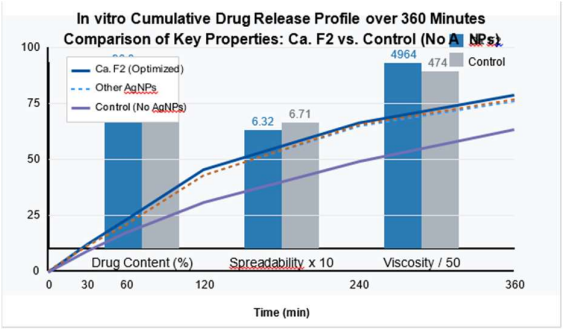

Figure 1: Grouped bar chart summarizing the physicochemical properties of the optimized formulation (Ca. F2) versus the control batch lacking silver nanoparticles. Note: Spreadability and viscosity values were scaled for graphical visualization.

4.5 *In vitro* Drug Release

The cumulative drug release profiles over 360 minutes, determined using a Franz diffusion cell, are detailed in Table 4 and visualized in Figure 2. Formulations containing AgNPs significantly outperformed the control batch. The optimized Ca. F2 formulation achieved the highest cumulative release (79.04%), owing to the increased surface area provided by the nanoparticles and the solubilizing effect of the PEG 6000 coating, facilitating effective diffusion across the membrane.

Table 4: In vitro Cumulative Drug Release (%)

Time (min)	Ca. F1	Ca. F2	Ca. F3	HPMC F1	HPMC F2	HPMC F3	Control (No AgNPs)
30	11.51	12.32	11.91	11.23	11.10	11.56	9.34
60	20.89	23.33	21.51	20.08	20.69	21.10	17.57
120	42.93	45.75	43.34	43.14	42.73	43.55	31.11
240	64.97	66.61	65.18	64.57	65.38	64.97	49.40
360	76.20	79.04	77.42	76.40	76.81	76.01	63.67

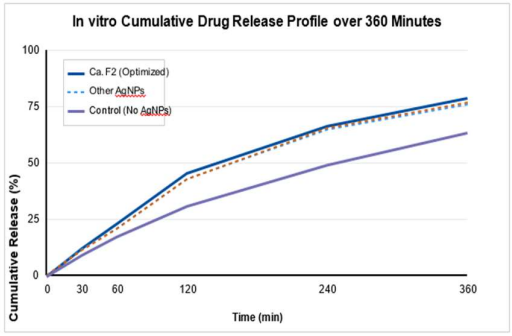

Figure 2: In vitro drug release profile showing the superior cumulative release of the optimized Ca. F2 formulation compared to other test batches and the non-nanoparticle control.

4.6 Antifungal Activity

The antifungal efficacy against *Candida albicans* was robustly correlated with the formulation strategy. The agar well-diffusion method demonstrated a profound synergistic effect when LZL was combined with AgNPs. The pure drug elicited a minimal zone of inhibition (8 mm). The formulation without silver nanoparticles slightly improved this to 11 mm, likely due to enhanced hydration from the gel. However, the incorporation of AgNPs caused a dramatic increase in efficacy. The optimized Ca. F2 formulation displayed an unprecedented zone of inhibition of 33 mm (Figure 3). HPMC formulations also performed well but were outmatched by their Carbopol counterparts (e.g., HPMC F2 achieved 27 mm).

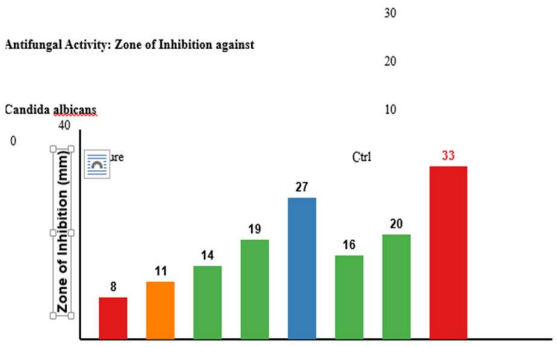

Figure 3: Bar chart displaying the substantial increase in the zone of inhibition achieved by the optimized Ca. F2 formulation, highlighting the synergistic antifungal effect of LZL and AgNPs.

5. Discussion

The successful formulation of a topical drug delivery system for a BCS Class II API requires overcoming the inherent barrier of low aqueous solubility. This study addressed this by utilizing a multi-faceted approach. First, the green synthesis of silver nanoparticles provided a stable, highly active component. The conversion of $AgNO_3$ utilizing *Epipremnum aureum* extract proved efficient, fast (30 min at 70 °C), and environmentally benign, yielding particles with an ideal mean size of 141.7 nm. A zeta potential of -25.9 mV indicated high colloidal stability imparted by the capping phytochemicals [10, 11].

Secondly, PEGylation (using PEG 6000) of the LZL and its subsequent integration with the AgNPs produced an advanced nanogel delivery vehicle. PEG serves a dual purpose: it acts as a hydrophilic carrier, converting crystalline LZL into an amorphous state (as confirmed by the DSC thermogram shift from 154 °C to 112 °C), thereby increasing its dissolution velocity [12]. Simultaneously, PEG provides steric hindrance preventing AgNP aggregation, which explains the high negative zeta potential (-44.7 mV) observed in the optimized Ca. F2 hydrogel.

Carbopol 940 proved to be a superior gelling matrix compared to HPMC K100 in terms of stabilizing the nanoparticle suspension and controlling drug release. At a 3% concentration (Batch Ca. F2), Carbopol generated an optimal viscosity of 4964 cps and a spreadability of 6.32 g·cm/sec, creating a film that adheres well to the skin without running. The resulting *in vitro* release demonstrated near 80% permeation over 6 hours. This marks a massive improvement over traditional cream bases which often restrict drug liberation.

The most consequential finding was the biological evaluation. The resistance of *Candida* species to azole antifungals relies heavily on alterations in the ergosterol pathway and the upregulation of efflux pumps [2]. AgNPs, however, operate via completely different mechanisms, primarily targeting the structural integrity of the cell membrane and disrupting intracellular metabolism [7].

By delivering Luliconazole, which inhibits lanosterol 14α-demethylase, simultaneously with cell-wall-destroying AgNPs directly to the infection site, the hydrogel bypasses conventional resistance pathways. This is unequivocally demonstrated by the Ca. F2 batch's 33 mm zone of inhibition, a fourfold increase over the pure drug.

6. Conclusion

The present investigation successfully developed, optimized, and evaluated a novel topical hydrogel system containing Luliconazole and green-synthesized silver nanoparticles. Utilizing *Epipremnum aureum* leaf extract for AgNP synthesis provided an eco-friendly and stable nanoparticle core. PEG 6000 was highly effective in improving the aqueous solubility of the BCS Class II drug and maintaining colloidal stability. The optimized Carbopol 940 (3%) formulation, Ca. F2, possessed excellent physicochemical characteristics, sustained drug release properties, and unparalleled antifungal efficacy against *Candida albicans* (33 mm zone of inhibition). This combinatorial nanotechnology platform offers a highly promising, biocompatible, and synergistic therapeutic approach to combat resistant topical dermatophytic and candidal infections, warranting further *in vivo* and clinical exploration.

References

1. [1] Prajapati ST, Patel CG, Patel CN. Formulation and evaluation of transdermal patch of repaglinide. ISRN Pharm. 2011;2011:651909.
2. [2] Lee Y, Puumala E, Robbins N, Cowen LE. Antifungal Drug Resistance: Molecular Mechanisms in Candida albicans and Beyond. Chem Rev. 2020;121(6):3390-3411.
3. [3] Khanna D, Bharti S. Luliconazole for the treatment of fungal infections: an evidence-based review. Core Evid. 2014;9:113-124.
4. [4] Bseiso EA, Nasr M, Sammour O, Abd El Gawad N. Recent advances in topical formulation carriers of antifungal agents. Indian J Dermatol Venereol Leprol. 2015;81(5):457-463.
5. [5] Savjani KT, Anuradha K, Gajra B. Drug solubility: importance and enhancement techniques. ISRN Pharm. 2012;2012:195727.
6. [6] Burdușel AC, Gherasim O, Grumezescu AM, Mogocea L, Ficai A, Andronescu E. Biomedical Applications of Silver Nanoparticles: An Up-to-Date Overview. Nanomaterials. 2018;8(9):681.
7. [7] Dakal TC, Kumar A, Majumdar RS, Yadav V. Mechanistic Basis of Antimicrobial Actions

of Silver Nanoparticles. Front Microbiol. 2016;6:1831.

8. [8] Yin IX, Zhang J, Zhao IS, Mei ML, Li Q, Chu CH. The Antibacterial Mechanism of Silver Nanoparticles and Its Application in Dentistry. Int J Nanomedicine. 2020;15:2555-2562.
9. [9] Panáček A, Kvítek L, Smékalová M, et al. Bacterial resistance to silver nanoparticles and how to overcome it. Nat Nanotechnol. 2018;13(1):65-71.
10. [10] Ali EAM. Antimicrobial activity, cytotoxicity, and phytochemicals screenings of Epipremnum aureum extracts. Egypt J Exp Biol. 2018;14(2):239-247.
11. [11] Garibo D, Borbón-Nuñez HA, de León JND, et al. Green synthesis of silver nanoparticles using plant extracts exhibit high-antimicrobial activity. Sci Rep. 2020;10(1):12805.
12. [12] Tejamaya M, Römer I, Merrifield RC, Lead JR. Stability of citrate, PVP, and PEG coated silver nanoparticles in ecotoxicology media. Environ Sci Technol. 2012;46(13):7011-7017.
13. [13] Pinzaru I, Coricovac D, Dehelean C, et al. Stable PEG-coated silver nanoparticles–A comprehensive toxicological profile. Food Chem Toxicol. 2018;111:546-556.
14. [14] Jain S, Patel N, Madan P, Lin S. Formulation and rheological evaluation of ethosome-loaded carbopol hydrogel for transdermal application. Drug Dev Ind Pharm. 2016;42(8):1315-1324.
15. [15] Çağlar EŞ, Güven GK, Okur NÜ. Preparation and characterization of carbopol based hydrogels containing dexpanthenol. J Fac Pharm. 2023;11(2):123-134.
16. [16] Shokri A, Abastabar M, Keighobadi M, et al. Promising antileishmanial activity of novel imidazole antifungal drug luliconazole. J Glob Antimicrob Resist. 2018;14:260-264.
17. [17] Alibakhshi A, Amini M, Asadi F. Development and evaluation of niosomal gels for topical delivery of luliconazole. J Liposome Res. 2021;31(2):185-193.
18. [18] Dandagi PM, Pandey P, Gadad AP. Formulation and evaluation of microemulsion based luliconazole gel for topical delivery. Indian J Pharm Educ Res. 2020;54(3):641-650
19. [19] Hawar SN, Al-Shmgani HS, Al-Kubaisi ZA. Green Synthesis of Silver Nanoparticles from Alhagi graecorum Leaf Extract and Evaluation of Their Cytotoxicity and Antifungal Activity. J Nanomater. 2022;2022:1058119.
20. [20] Loo YY, Rukayadi Y, Nor-Khaizura MAR. In Vitro Antimicrobial Activity of Green Synthesized Silver Nanoparticles. Front Microbiol. 2018;9:1555.
21. [21] Rout Y, Behera S, Ojha AK. Green synthesis of silver nanoparticles using Ocimum sanctum and study of their antibacterial and antifungal activities. J Microbiol Antimicrob. 2012;4(6):103-109.
22. [22] Radziuk D, Skirtach A, Sukhorukov G. Stabilization of silver nanoparticles by polyelectrolytes and poly (ethylene glycol). Macromol Rapid Commun. 2007;28(8):848-855.
23. [23] Slepička P, Elashnikov R, Ulbrich P. Stabilization of sputtered gold and silver nanoparticles in PEG colloid solutions. J Nanopart Res. 2015;17(5):224.
24. [24] Manson J, Kumar D, Meenan BJ, Dixon D. Polyethylene glycol functionalized gold nanoparticles: the influence of capping density on stability. Gold Bull. 2011;44(2):99-105.
25. [25] Roy A, Bulut O, Some S, Mandal AK, Yilmaz MD. Green synthesis of silver nanoparticles: biomolecule-nanoparticle organizations targeting antimicrobial activity. RSC Adv. 2019;9(5):2673-2702.
26. [26] Smitha SL, Nissamudeen KM, Philip D. Studies on surface plasmon resonance and optical properties of silver nanoparticles. Spectrochim Acta A Mol Biomol Spectrosc. 2008;71(1):186-190.
27. [27] Bhattacharjee S. DLS and zeta potential–what they are and what they are not? J Control Release. 2016;235:337-351.
28. [28] Bao Q, Newman B, Wang Y, Choi S. In vitro and ex vivo correlation of drug release from ophthalmic ointments using Franz diffusion cells. J Control Release. 2018;276:114-123.
29. [29] Masomi F, Hassanshahian M. Antimicrobial activity of five medicinal plants on Candida albicans evaluated by agar well diffusion. Iran J Toxicol. 2016;10(2):29-33.
30. [30] Rahdar A, Amini N, Askari F. Dynamic light scattering: A useful technique to characterize nanoparticles. J Nanopart Res. 2019;21(3):1-10.
31. [31] Vanden Bossche H. Mechanisms of antifungal resistance. Rev Iberoam Micol. 1997;14(2):44-49.
32. [32] Mubarak TH. Surface Plasmon Resonance of Silver Nanoparticles: Synthesis and Characterization. J Biochem Tech. 2019;10(2):45-51.
33. [33] Folzer E, Gonzalez D, Singh R. Comparison of skin permeability for topical formulations: an in vitro study. J Pharm Sci. 2014;103(1):1-10.
34. [34] Alzoubi FY. Localize surface plasmon resonance of silver nanoparticles. J Mater Sci Mater Electron. 2023;34(1):12-19.

35. [35] Sharma P, Patel K. Drug-Excipient Compatibility Studies: First Step for Dosage Form Development using FTIR and DSC. Pharm Innov J. 2022;11(1):234-245.